

Performance Analysis of Medical Image Segmentation and Edge Detection using MEM and PSO Algorithms

R. Harikumar¹ and B. Vinoth Kumar^{2,*}

¹ Department of ECE, Bannari Amman Institute of Technology, Sathyamangalam, India

² Department of EEE, Bannari Amman Institute of Technology, Sathyamangalam, India.

Received: 13 Mar. 2015, Revised: 11 May 2015, Accepted: 12 May 2015

Published online: 1 Nov. 2015

Abstract: This study evaluates the performance of quality measures for the algorithms Modified Expectation Maximization (MEM) and Particle Swarm Optimization (PSO) in segmentation of medical images. Medical images of different modalities, such as computed tomography, magnetic resonance, X-ray and ultrasonic are considered for this study. The quality measures like peak signal to noise ratio (PSNR), average difference (AD), structural content (SC), image fidelity (IF), normalized correlation coefficient (NK), mean structural similarity index (MSSIM) and universal quality index (UQI) are calculated for medical images using MEM and PSO method. Experimental results sound profound for Modified Expectation Maximization (MEM) with average of 3dB increase in PSNR values than the PSO. Also, Figure of Merit (FOM) a performance measure for edge detection is considered for choosing the best technique of edge detection for medical images. Finally, Trend factor is set using aggregated quality values and FOM for the better segmentation as well as edge detection.

Keywords: Segmentation, K-means clustering, MEM, PSO, Edge Detector, Quality measures

1 Introduction

In Digital Image Processing, Segmentation is a crucial process which has found wide applications in areas such as medical image processing, compression, diagnosis arthritis from joint image [1,2], automatic text hand writing analysis [3] and remote sensing. Segmenting medical images is very important for detecting abnormalities, studying and tracking progress of diseases, and surgery planning. Medical image segmentation is a tricky problem due to the fact that medical images commonly have poor contrasts, different types of noise, and missing or diffuse boundaries. Medical image segmentation is an important but difficult problem that attracts tremendous attentions of researchers from various fields. Automatic segmentation of medical images is a difficult task as medical images are complex in nature and rarely have any simple linear feature. Although a number of algorithms have been proposed in the field of medical image segmentation, medical image segmentation continues to be a complex and challenging problem. As we know, the output of segmentation algorithm is deviant due to partial volume effect, intensity in homogeneity,

presence of artifacts and closeness in gray level of different soft tissue. These approaches include local edge detection [4], deformable curves [5], morphological region-based approaches [6,7], global optimization approaches on energy functions and stochastic model-based methods [8,9]. Some intensity-based methods such as thresholding and histogram-based finite mixture models are easy to be formulated and fast. However they often fail to segment objects with low contrast or noisy images with varying background. It is noted that these methods don't use the spatial morphological images information [10]. On the other hand, some other methods such as morphological segmentation, region growing and deformable curves, mainly focus on spatial information such as local structures or regions.

In supervised approach, it is usually assumed that training data are available for the image classes; therefore, the parameters can be estimated from the training data before segmentation. For unsupervised techniques, the objective is to estimate the parameters and segment the image simultaneously [11]. Most of the proposed solutions to the unsupervised segmentation problem can

* Corresponding author e-mail: bojanvinoth@gmail.com

be classified into two broad categories; one is a two-step procedure, estimating the parameters for each class and then using a relaxation scheme to do segmentation [12].

An optimal initialization method based on Particle swarm optimization (PSO) algorithm approach, for a better unsupervised medical image segmentation has been taken for study.

A Modified Expectation Maximization (MEM) model was utilized for segmentation of medical images. The quality measures are calculated for both the methods and their efficacy are reported. Additionally, three edge detection techniques such as Sobel, canny and principal component analysis are compared with one another so as to choose the better technique for edge detection in medical image.

Section 2, presents methodology for the Modified Expectation Maximization (MEM) algorithm and Particle swarm optimization PSO for optimization of clusters are analyzed. In section 3, Edge detection and preservation techniques are elucidated. Section 4, gives the outline on quality measures. In section 5, experimental results for both MEM and PSO based on quality measures and trend factor are analyzed. The paper is concluded in section 6 with a note on research challenges in medical segmentation.

2 Material and Methods

The main objective of this research is depicted in the flow chart as shown in Fig. 1. The flow chart shows that the basic process of segmentation is K -means clustering and the tightness of clusters (i.e.) intra distance of the clusters are modified using the principles of MEM and PSO. Three types of edge detection algorithms such as PCA, Sobel and Canny operators are used to identify the true edges of the images. From the parameters (i.e.) Figure of merit (FOM) and aggregation of quality measures, the trend factor is set up. A constrain of trend factor in the range between lower bound (LB) and upper bound (UB) is set, other than that leads to modification of the cluster centre of k -means and the entire process is repeated once again. Otherwise, process is ended with segmented image.

2.1 General Techniques

In this part, a Maximum Likelihood (ML) approach which uses a Modified Expectation Maximization (MEM) algorithm for medical image segmentation is addressed. Similar to the conventional EM algorithm, this algorithm alternates between the estimation of the complete log-likelihood function (E-step) and the maximization of this estimate over values of the unknown parameters (M-step) [13]. Due to difficulties in the evaluation of the ML function [14], some modifications are made in the EM algorithm which is outlined below. Additionally, PSO

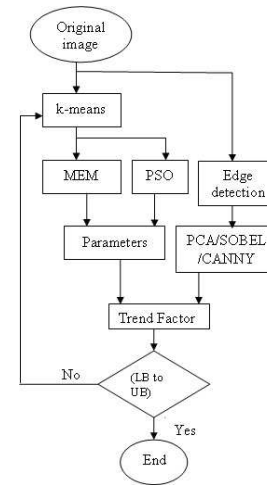


Fig. 1: Flow Chart depicting the Overall Segmentation process

(Particle Swarm Optimization) have been applied in order to achieve the collective behavior and optimization in cluster classification.

2.2 Maximum-Likelihood Estimation

Simplified steps of maximum likelihood estimation are drafted below:

- i) Find the parameters (i.e. means, covariances and mixing weights) of maximum likelihood estimation
- ii) Calculate the Euclidean Distance (d) assigning each x_i to its nearest cluster center c_k .
- iii) In maximization step use Maximum $Q(\theta, \theta')$, The likelihood function is written as:

$$Q(\theta^{i+1}, \theta^i) = \max Q(\theta^i, \theta), \theta^{i+1} = \arg \max Q(\theta, \theta^i) \quad (1)$$

$$d(p, q) = d(q, p) = \sqrt{\sum_{i=1}^n (q_i - p_i)^2} \quad (2)$$

- iv) Repeat iterations, and don't stop the loop until $\|\theta^{i+1} - \theta^i\|$ small enough.

The algorithm terminates when the difference between the log likelihood for the previous iteration and current iteration fulfills the tolerance [15]. The results of segmentation of medical images with MEM algorithm ($k = 8$) are discussed in section 5.

2.3 Particle Swarm Optimization (PSO)

Particle Swarm optimization is a optimization algorithm which developed by Eber hartand kennedy in 1995. The basic idea is that an N -dimensional search space is performed with help of agents (particles) and the best

position encountered by itself and its neighbor [16]. Each agent is deemed to occupy a position $(Xi(k))$ and velocity $vi(k)$

PSO Algorithm Outline:

Step 1: Each agents are assigned an initial position and initial velocity

Step 2: Update the position and velocity by local and global classification

Step 3: New values for the position an velocity are selected using equation (3) and (4).

$$X_{k+1}^i = X_k^i + v_{k+1}^i \tag{3}$$

$$v_{k+1}^i = v_k^i + c_1r_1(p_k^i - X_k^i) + c_2r_2(p_k^g - X_k^i) \tag{4}$$

Step 4: Step 2 and 3 are repeated until a convergence criterion is met.

The output of the segmentation of different types of medical images using PSO is shown in section 5. A relationship is identified between segmentation and true edges through trend factor as an aggregation of parameters. Therefore edge detection also leads to segmentation of the images.

3 Edge Detection as a Component For Segmentation

Edge detection refers to the process of identifying and locating sharp discontinuities in an image. The basic idea of edge detection is to extract and remove the edge point set. Former is done using edge operator and later some of the edge points from the edge point set are replaced with some another and lines are formed by linking the obtained edge point set. Three edge techniques such as PCA, Sobel and Canny are taken for study. FOM (Figure of Merit) comparison is done for different types of medical images using these techniques and the results are tabulated in Table 5.

3.1 Methodology for Edge Detection

A. Principal Component Analysis

Principal component analysis (Karhunen-Loeve or Hotelling transform) - PCA belongs to linear transforms based on the statistical techniques. This method provides a powerful tool for data analysis and pattern recognition which is often used in signal and image processing as a technique for data compression, data dimension reduction or their edge detection as well. The PCA algorithm is summarized as

Step 1: organize the input data set and calculate the mean using equation (5)

$$m_x \approx \frac{1}{L} \sum_{l=1}^L X_l \tag{5}$$

Step 2: Calculate the covariance matrix in order to find the eigen vectors and eigen values using equation (6) & (7)

$$C_x = \varepsilon\{(X - m_x)(X - m_x)^t\} \tag{6}$$

$$\approx \frac{1}{L} \sum_{l=1}^L X_l X_l^t - m_x m_x^t \tag{7}$$

Step 3: Compute cumulative energy content for each eigen vector in order to select a subset of eigen vector as basis vector

Step 4: Convert the source data set into new data set.

B. Sobel Edge Detector

The Sobel operator consists of a pair of 3×3 convolution kernels. One kernel is simply the other rotated by 90° . The kernels can be applied separately to the input image, to produce separate measurements of the gradient component in each orientation (call these G_x and G_y). These can then be combined together to find the absolute magnitude of the gradient at each point and the orientation of that gradient. The gradient magnitude is given by:

$$|G| = \sqrt{G_x^2 + G_y^2} \tag{8}$$

Typically, an approximate magnitude is computed using:

$$|G| = |G_x| + |G_y| \tag{9}$$

This is much faster to compute. The angle of orientation of the edge (relative to the pixel grid) giving rise to the spatial gradient is given by:

$$\text{Theta} = \arctan(G_y/G_x) \tag{10}$$

C. Canny Edge Detector

The algorithmic steps [17] for canny edge detection technique are follows:

1. Convolve the image with a two dimensional Gaussian filter to smooth it.
2. Differentiate the image in two orthogonal directions.
3. Calculate the gradient amplitude and direction.
4. Perform non-maximal suppression.
5. Any gradient value that is not a local peak is set to zero. The gradient direction is used in this process.
6. Threshold these edges to eliminate insignificant edges.

3.2 Pratt's Figure of Merit

Pratt's Figure of Merit (FOM) is one of the performance measures for edge detection. It attempts to balance three types of errors that can produce erroneous edge maps: missing valid edge points, failure to localize edge points and classification of noise fluctuations as edge points. The Figure of Merit is defined as

$$FOM = \frac{1}{I_N} \sum i = 1^L \frac{1}{1 + ad^2} \tag{11}$$

Where, I_N is the maximum of I_A and I_I . I_A represents the total number of actual edge pixels; i.e., those edge pixels that were found. I_I represents the total number of ideal pixels in the image; i.e., the number of edge pixels in the reference image. The Figure of Merit is normalized with the maximum of the actual and ideal number of edge pixels in order to ensure a penalty for smeared (i.e., $I_I < I_A$) or fragmented edges (i.e., $I_I > I_A$).

4 Quality Measures

To compare the performance analysis of MEM and PSO algorithms, quality measures that are described by I. Avicibas et. al [20], M. Mrak et. al [19] and A.M. Eskicioglu et. al [18] were taken. The outline of the quality measures are stated below.

4.1 Peak Signal To Noise Ratio (PSNR)

$$PSNR = 10 \log \frac{255 * 255}{MSE} dB \quad (12)$$

where MSE is mean square error [21]. Ideally it is infinity. Practically it is in the range of 25 to 40dB.

4.2 Average Difference (AD)

$$AD = \sum_{j=1}^M \sum_{k=1}^N [X(j,k) - \hat{X}(j,k)] / MN \quad (13)$$

This measure shows the average difference between the pixel values, ideally it should be zero.

4.3 Structural Content (SC), Image Fidelity (IF) and Normalized Correlation Coefficient (NK)

These are the co relational based quality measure which normally looks at correlation features between the pixels of original and reconstructed image, they are given as

$$SC = \frac{\sum_{j=1}^M \sum_{k=1}^N X(j,k)^2}{\sum_{j=1}^M \sum_{k=1}^N \hat{X}(j,k)^2} \quad (14)$$

$$IF = 1 - \frac{\sum_{j=1}^M \sum_{k=1}^N [X(j,k) - \hat{X}(j,k)]^2}{\sum_{j=1}^M \sum_{k=1}^N [X(j,k)]^2} \quad (15)$$

$$NK = 1 - \frac{\sum_{j=1}^M \sum_{k=1}^N [X(j,k)\hat{X}(j,k)]}{\sum_{j=1}^M \sum_{k=1}^N [X(j,k)]^2} \quad (16)$$

Normally SC , IF and NK are in the range of 0 to 1, very near to or one is the best.

4.4 Mean Structural Similarity Index (MSSIM) and Universal Quality Index (UQI)

Zhou Wang et. al [21] in their paper proposed a new quality measures, viz mean structural similarity index and universal quality index. This compares local patterns of pixel intensities that have been normalized for luminance and contrast. It is given by

$$SSIM = \frac{(2\mu_x\mu_y + C_1)(2\sigma_{xy} + C_2)}{(\mu_x^2 + \mu_y^2 + C_1)(\sigma_x^2 + \sigma_y^2 + C_2)} \quad (17)$$

Where μ and σ are mean and variance respectively, x and y are for original and segmented images. The MSSIM is calculated by taking mean of SSIM and UQI is calculated by substituting the values of C_1 and C_2 as zero.

5 Results and Discussion

An analysis is done on segmentation of medical images by intriguing MRI images, X-ray images, CT images and Ultrasonic images. We have approached our problem in three phases. a) To perform segmentation of medical images using MEM and PSO algorithm. b) To compare edge detection techniques (PCA/Sobel/Canny) for the chosen medical images using FOM (Figure of merit). c) Finally, parameters from the two phases are investigated using trend factor. The segmented output of medical images using Modified Expectation Maximization (MEM) method for the different cluster size were performed for MRI image, CT image, X-ray image and Ultrasonic image which are depicted in Fig. 2. Similarly, the segmented output of medical images using Particle Swarm Optimization (PSO) method for the different cluster size was performed for MRI image, CT image, X-ray image and Ultrasonic image which are depicted in Fig. 3. Performance analysis on medical image segmentation were performed by both MEM and PSO methods using quality measures [20,19,18] (PSNR, Average difference(AD), structural content (SC), image fidelity (IF), normalized correlation coefficient (NK) mean structural similarity index (MSSIM) and universal quality index (UQI)) and results are tabulated in Table 2, Table 3 and Table 4.

It is observed that average of 3dB increment of PSNR values in MEM models when compared to PSO algorithm techniques. Higher Average difference in PSO models indicates intra cluster fragileness. The performance measures of edge detection techniques (PCA/Sobel/Canny) for the chosen medical images such as MRI, X-ray, CT and Ultrasonic are premeditated using equation (11). The Table 5 shows the Figure of Merit (FOM) for different types of medical images.

Table 1: Quality Measures of MRI Images

IQM	MRI																			
	IMAGE QUALITY MEASUREMENT VALUE																			
	BRAIN										CARDIAC									
	MBM					PSD					MBM					PSD				
k=4	k=5	k=6	k=7	k=8	k=4	k=5	k=6	k=7	k=8	k=4	k=5	k=6	k=7	k=8	k=4	k=5	k=6	k=7	k=8	
PSNR	32.8063	34.7631	35.1227	36.1435	36.7481	26.8668	26.9644	27.5871	27.9222	28.2244	34.1071	34.0546	35.1237	35.5387	37.2301	26.7348	26.9119	27.9645	27.9865	28.1099
AD	15.8151	14.0027	11.2743	9.9613	8.7372	14.2578	11.6694	9.844	8.8066	9.9441	23.349	18.0326	15.0914	11.8853	10.2191	17.2065	14.2251	11.4988	10.3101	9.6118
SC	0.9323	0.9258	0.9616	0.9544	0.9631	1.5182	1.3848	1.3201	1.2728	1.2607	0.8337	0.8915	0.8127	0.9496	0.9509	1.748	1.5165	1.4485	1.3524	1.2957
NK	0.9911	1.0095	0.9979	1.0073	1.0062	0.8043	0.8440	0.9666	0.883	0.8809	1.0177	1.0062	1.0093	0.9997	1.0084	0.7401	0.8005	0.8239	0.8542	0.873
IF	1.0645	1.0721	1.0318	1.0397	1.0302	0.6605	0.714	0.7494	0.7776	0.7851	1.1916	1.1139	1.0877	1.0453	1.0438	0.5642	0.6515	0.6825	0.7316	0.7639
SSIM	0.8943	0.9329	0.9507	0.9639	0.9719	0.9406	0.9628	0.9725	0.978	0.9648	0.8537	0.8994	0.9278	0.9485	0.9627	0.8808	0.926	0.9488	0.9625	0.9691
UQI	0.8935	0.9324	0.9503	0.9636	0.9717	0.9403	0.9626	0.9724	0.9779	0.9646	0.8529	0.8978	0.9274	0.9482	0.9625	0.8803	0.9257	0.9485	0.9624	0.969
	KNEE										SIDEHEAD									
	MBM					PSD					MBM					PSD				
	k=4	k=5	k=6	k=7	k=8	k=4	k=5	k=6	k=7	k=8	k=4	k=5	k=6	k=7	k=8	k=4	k=5	k=6	k=7	k=8
PSNR	30.5665	31.4139	32.1911	32.84	33.9244	26.2836	26.5681	26.7822	27.0257	27.3342	30.6008	31.89	32.5945	32.8115	33.7009	26.2331	26.4729	26.7556	27.1181	27.4468
AD	14.7824	12.3668	10.4366	8.5823	7.5235	22.4077	18.167	14.9925	12.9584	11.4243	14.5994	12.5066	10.7293	8.3267	7.1077	24.7744	18.6572	15.3959	13.0478	11.6849
SC	1.0343	1.0269	1.0208	1.0188	1.0129	1.557	1.439	1.3276	1.2656	1.2347	1.0298	1.0196	1.0135	1.0289	1.0259	1.7238	1.4973	1.3818	1.3027	1.2671
NK	0.9474	0.9628	0.9728	0.9787	0.9848	0.7878	0.8279	0.8621	0.8846	0.8968	0.945	0.9635	0.9743	0.9725	0.9777	0.7478	0.8103	0.8458	0.8723	0.8854
IF	0.961	0.968	0.9738	0.9759	0.9815	0.6364	0.6939	0.7474	0.7843	0.8041	0.9648	0.9744	0.9803	0.9655	0.9684	0.5738	0.6614	0.7172	0.7612	0.7828
SSIM	0.9164	0.946	0.9507	0.9628	0.9739	0.9812	0.9199	0.9488	0.967	0.9764	0.982	0.987	0.9352	0.9556	0.9688	0.8959	0.9493	0.9634	0.9743	0.9829
UQI	0.916	0.9468	0.9627	0.9738	0.9811	0.9197	0.9487	0.9669	0.9764	0.982	0.8964	0.9340	0.9564	0.9687	0.9778	0.8956	0.9442	0.9633	0.9743	0.9797

Table 2: Quality Measures of X-ray Images

IQM	X-RAY																			
	IMAGE QUALITY MEASUREMENT VALUE																			
	CHEST										TEETH									
	MBM					PSD					MBM					PSD				
k=4	k=5	k=6	k=7	k=8	k=4	k=5	k=6	k=7	k=8	k=4	k=5	k=6	k=7	k=8	k=4	k=5	k=6	k=7	k=8	
PSNR	30.1053	30.1588	31.283	32.2486	32.9822	24.6541	24.8207	25.1664	25.521	25.9515	30.3073	30.5283	31.388	31.6976	33.4461	25.1015	25.4623	25.4121	25.8433	26.2341
AD	3.0505	0.4940	0.2239	0.0356	0.2371	31.5655	25.4927	20.8359	17.7783	15.239	3.2044	1.4697	1.2733	0.8427	0.4239	25.8273	20.4123	19.6434	15.8261	13.8052
SC	1.0127	1.0336	1.0244	1.0109	1.0083	1.5339	1.3879	1.3162	1.2509	1.2288	0.9913	1.0094	1.0040	1.0076	0.024	1.4173	1.3478	1.3296	1.246	1.2034
NK	0.9844	0.9782	0.9346	0.9921	0.9939	0.7866	0.8348	0.8625	0.8867	0.8987	1.995	1.9599	0.9933	0.9927	0.9962	0.8282	0.8547	0.8623	0.8823	0.9088
IF	0.9808	0.9607	0.9595	0.9825	0.9851	0.6452	0.7138	0.753	0.7927	0.8124	1.0022	0.9842	0.9882	0.986	0.9911	0.6991	0.7355	0.7466	0.7961	0.8245
SSIM	0.9638	0.9788	0.9867	0.9909	0.9929	0.9155	0.9473	0.9641	0.973	0.9793	0.9402	0.9595	0.9716	0.9781	0.9839	0.9324	0.951	0.9627	0.9756	0.9823
UQI	0.9635	0.9787	0.9866	0.9908	0.9928	0.9153	0.9472	0.964	0.973	0.9793	0.9397	0.9591	0.9714	0.9779	0.9838	0.932	0.9507	0.9625	0.9757	0.9822
	HAND										SKULL									
	MBM					PSD					MBM					PSD				
	k=4	k=5	k=6	k=7	k=8	k=4	k=5	k=6	k=7	k=8	k=4	k=5	k=6	k=7	k=8	k=4	k=5	k=6	k=7	k=8
PSNR	33.9256	34.3006	35.0334	35.7506	36.6378	30.1532	30.4663	30.8861	30.9827	31.1966	33.612	34.4024	34.8633	36.436	38.215	27.1634	27.507	27.9369	28.0463	28.0267
AD	35.2508	29.4244	25.2235	21.7349	19.0491	10.0054	7.8954	6.2887	5.3449	4.6069	19.9706	16.7662	13.1961	11.2772	10.3125	15.7958	12.181	10.1081	8.7011	9.3148
SC	0.8765	0.9247	0.949	0.9631	0.9701	1.5442	1.4433	1.3249	1.2646	1.2049	0.9026	0.9228	0.9607	0.9728	0.966	1.5572	1.3388	1.3016	1.2381	1.2577
NK	0.9361	0.9465	0.9583	0.9685	0.9771	0.7915	0.8258	0.8644	0.886	0.9081	1.0061	1.0083	0.9923	0.9968	0.042	0.7923	0.8481	0.8723	0.896	0.8882
IF	1.1355	1.078	1.0483	1.0329	1.0254	0.6421	0.6874	0.7493	0.7853	0.8245	1.0009	1.0767	1.034	1.021	0.283	0.6352	0.7236	0.7613	0.8007	0.7981
SSIM	0.7575	0.814	0.8553	0.8865	0.9095	0.9223	0.9521	0.9709	0.9793	0.9861	0.8065	0.9346	0.9537	0.9658	0.9736	0.9313	0.9307	0.9735	0.9828	0.9792
UQI	0.7569	0.8143	0.8549	0.8862	0.9093	0.9222	0.952	0.9707	0.9792	0.985	0.906	0.9343	0.9535	0.9656	0.9735	0.931	0.9306	0.9734	0.9828	0.9791

Table 3: Quality Measures of CT Images

IQM	CT																			
	IMAGE QUALITY MEASUREMENT VALUE																			
	BRAIN										SPINE									
	MBM					PSD					MBM					PSD				
k=4	k=5	k=6	k=7	k=8	k=4	k=5	k=6	k=7	k=8	k=4	k=5	k=6	k=7	k=8	k=4	k=5	k=6	k=7	k=8	
PSNR	33.1939	33.2316	34.2898	31.8159	34.8554	25.6237	25.6537	26.8918	26.7919	26.7435	28.1879	31.2687	31.978	33.1228	32.2971	24.5146	26.3157	26.3052	26.5176	26.7813
AD	21.5284	1.9064	13.5425	7.2873	8.3984	22.9685	20.4985	17.3845	12.556	11.7883	1.6017	5.2417	3.2789	2.078	1.4979	29.9606	15.4483	14.3487	13.338	12.745
SC	0.9255	0.8807	0.9826	1.0805	1.0116	1.7563	1.5513	1.5144	1.3334	1.2856	1.0681	0.9165	0.9552	0.9992	0.9997	2.4402	1.5433	1.4684	1.3872	1.3473
NK	0.9935	0.9331	0.9881	0.948	0.9841	0.7481	0.7959	0.8079	0.8639	0.88	0.8378	1.0218	1.0083	0.9891	0.9904	0.6195	0.7937	0.819	0.8402	0.8524
IF	1.0741	0.9189	1.0113	0.9191	0.9821	0.563	0.6336	0.6539	0.7438	0.7714	0.9252	1.0801	1.0358	0.9898	0.9892	0.3987	0.3369	0.6748	0.7098	0.7311
SSIM	0.9016	0.9289	0.9362	0.9662	0.9784	0.908	0.9348	0.9468	0.9747	0.9797	0.8535	0.8929	0.93	0.9441	0.9529	0.7949	0.9132	0.9387	0.9498	0.9538
UQI	0.9011	0.9285	0.956	0.966	0.9783	0.9077	0.9347	0.9467	0.9746	0.9797	0.8493	0.8906	0.9285	0.9428	0.9518	0.793	0.9119	0.9379	0.9491	0.9532
	LUNG										EOSINOPHUC									
	MBM					PSD					MBM					PSD				
	k=4	k=5	k=6	k=7	k=8	k=4	k=5	k=6	k=7	k=8	k=4	k=5	k=6	k=7	k=8	k=4	k=5	k=6	k=7	k=8
PSNR	33.5494	34.2796	36.3062	37.6149	38.4188	27.5576	28.2874	27.0903	27.8697	28.289	32.5136	32.5749	34.4107	34.3312	36.3486	27.8434	27.3316	27.754	28.6036	28.8674
AD	19.6227	6.051	14.1369	12.0622	10.5332	14.0111	10.0889	19.5731	11.591	10.8598	25.7036	20.4432	18.1303	14.9101	13.4598	16.0094	13.4935	11.9916	8.8796	7.8218
SC	0.9149	0.9461	0.9519	0.9665	0.9781	1.4431	1.2835	1.8043	1.3851	1.3014	0.9133	0.9708	0.9626	0.9848	0.9769	1.6283	1.4498	1.3922	1.2896	1.2373
NK	1	0.9863	1.0019	1	0.9977	0.8203	0.8739	0.7331	0.8435	0.8673	0.9751	0.9662	0.9844	0.982	0.9927	0.7729	0.8216	0.8423	0.8788	0.8964
IF	1.0859	0.9498	1.0434	1.0275	1.0152	0.6868	0.7712	0.5471	0.7148	0.7612	1.0862	1.0238	1.0325	1.0091	1.0173	0.6078	0.8304	0.712	0.7715	0.8019
SSIM	0.9039	0.9332	0.9625	0.9647	0.9723	0.9398	0.9675	0.9806	0.9602	0.9627	0.8646	0.9042	0.9323	0.9497	0.9626	0.9181	0.9459	0.9608	0.9775	0.9831
UQI	0.9034	0.9329	0.9623	0.9646	0.9722	0.9395	0.9673	0.8901	0.96	0.9625	0.864	0.9038	0.9321	0.9495	0.9625	0.9178	0.9467	0.9607	0.9774	0.9831

Table 4: Quality Measures of Ultrasonic Images

IQM	ULTRASONIC																			
	IMAGE QUALITY MEASUREMENT VALUE																			
	BABY										SPINE									
	MEM					PSO					MEM					PSO				
k=4	k=5	k=6	k=7	k=8	k=4	k=5	k=6	k=7	k=8	k=4	k=5	k=6	k=7	k=8	k=4	k=5	k=6	k=7	k=8	
PSNR	27.1897	27.3937	27.5864	27.5914	27.7398	24.3959	24.512	24.805	24.5399	24.8282	33.4009	34.2226	35.2057	35.1489	36.275	26.9346	27.2474	27.5668	28.1198	28.6836
AD	15.2589	13.667	12.3344	11.5013	10.0535	37.4387	30.4466	25.8151	22.7442	20.136	21.9721	17.4783	14.3633	11.2399	9.6497	15.5611	12.3517	11.0077	9.2733	8.0268
SC	1.338	1.2765	1.2316	1.1989	1.1687	1.4819	1.3568	1.2842	1.2509	1.2016	0.7964	0.8501	0.883	0.9251	0.9364	1.8927	1.3486	1.5202	1.4279	1.3475
NK	0.8571	0.8803	0.8977	0.9109	0.923	0.8112	0.8511	0.8767	0.8902	0.9082	1.0163	1.0125	1.013	1.0023	1.0066	0.7074	0.7663	0.8025	0.8313	0.8574
IF	0.7425	0.7785	0.807	0.8292	0.8607	0.6899	0.7321	0.7738	0.7946	0.8273	1.2475	1.1666	1.1227	1.0711	1.0581	0.5185	0.5868	0.648	0.6905	0.7323
SSIM	0.9297	0.9556	0.9696	0.9789	0.9839	0.9472	0.9668	0.9757	0.9823	0.9847	0.7909	0.856	0.8978	0.925	0.9443	0.8574	0.9096	0.9368	0.956	0.9687
UQI	0.9294	0.9554	0.9695	0.9789	0.9839	0.9472	0.9668	0.9757	0.9822	0.9847	0.7887	0.8545	0.8967	0.9243	0.9438	0.8563	0.909	0.9368	0.9557	0.9685
IQM	ULTRASONIC																			
	IMAGE QUALITY MEASUREMENT VALUE																			
	BABY										SPINE									
	MEM					PSO					MEM					PSO				
k=4	k=5	k=6	k=7	k=8	k=4	k=5	k=6	k=7	k=8	k=4	k=5	k=6	k=7	k=8	k=4	k=5	k=6	k=7	k=8	
PSNR	31.4331	32.3021	33.3449	34.5721	35.3918	26.2138	26.7043	27.064	27.7199	28.4309	33.2221	34.1806	35.2282	37.1983	37.9513	26.1599	26.914	28.0178	27.8809	29.9901
AD	13.0415	10.9516	9.2428	7.9685	6.9028	18.2271	13.8972	11.5868	9.7453	8.462	6.1995	4.003	3.0142	2.7353	1.8873	13.9007	11.4068	9.5341	9.9234	7.3667
SC	0.8819	0.9013	0.9305	0.9442	0.9617	1.9054	1.6095	1.4764	1.3774	1.3288	0.9166	0.9511	0.969	0.9563	0.9868	1.6506	1.4716	1.3792	1.4673	1.2775
NK	0.9917	1.0025	0.9999	1.0023	0.9982	0.7034	0.7752	0.8148	0.8469	0.864	1.013	1.0061	1.0024	1.0078	1.0004	0.7657	0.8154	0.8461	0.8258	0.8817
IF	1.1231	1.0938	1.064	1.0484	1.029	0.5141	0.6106	0.6666	0.7152	0.7418	1.017	1.0374	1.018	1.0209	1.0004	0.5918	0.3655	0.7111	0.6722	0.7688
SSIM	0.7989	0.9649	0.9634	0.9308	0.9449	0.8517	0.9141	0.9439	0.9607	0.9721	0.8796	0.9283	0.9502	0.9358	0.9756	0.9119	0.3463	0.9644	0.9626	0.9798
UQI	0.7956	0.9628	0.902	0.9298	0.9441	0.8504	0.9133	0.9434	0.9603	0.9719	0.8756	0.9261	0.9487	0.9348	0.9748	0.9105	0.3446	0.9638	0.962	0.9795

Table 5: FOM for Medical Images

IMAGE	PCA	SOBEL	CANNY
MRI	0.4725	0.6169	0.7146
X-RAY	0.5217	0.5321	0.639
CT	0.5113	0.7393	0.7171
ULTRASONIC	0.5566	0.874	0.7637

5.1 Trend factor

In order to achieve a singleton decision about whether the clusters are formed in a right manner, a computation of quality parameters through an aggregation process is initiated. This parameter is known as trend factor and defined as

$$Trend\ factor(TF) = \frac{Aggregated\ Quality\ value(AQV)}{Min(FOM)} \tag{18}$$

where aggregated quality value(AQV) is defined as

$$AQV = w_1SC + w_2NK + w_3IF + w_4SSIM + w_5UQI \tag{19}$$

with weights as, $\sum_{i=1}^4 w_i = 1$. The determination of aggregation function is well discussed in [22] and [23]. In [23], Yager introduced the Ordered Weighed Averaging Aggregation (OWA) operator which models the max, min and arithmetic mean operators for certain vectors of weight (w_i). Selection of weights w_i are done in such a way to obtain the better scores for aggregation. Trend factor is bounded between lower bound (LB) and upper bound (UB) values. Lower bound (LB) is given by

$$LB = \min(y_1) = x^T w \tag{20}$$

where x is quality measure variable

$$y_1 = w_1x_1 + w_2x_2 + w_3x_3 + w_4x_4 + w_5x_5 \tag{21}$$

Upper bound (UB) is given by

$$UB = \max(y_1) = y'_1 \tag{22}$$

Trend factor results are tabulated in Table 6. The results indicate that PSO method with canny edge detector preserves more true edges than process through MEM. Even though PSNR values of MEM algorithm are higher than PSO, it does not guarantee the edge preservation of medical images. From this study, we conclude that PSO with canny operator may be well suited for better segmentation and edge detection.

6 Conclusion

In this paper, quality measures for segmentation of medical images using MEM and PSO algorithm are evaluated. An appropriate edge detection technique is chosen using Figure of Merit (FOM). The efficacy of trend factor chooses the best of the chosen methods for better segmentation as well as edge detection. The future direction of this research will be vector angle measure for edge detection and heuristic approaches for better edge preservation and compactness of cluster at larger size.

Table 6: Trend factor

MRI image	MEM	PSO	CT image	MEM	PSO
Cardiac	2.0905	2.1449	Brain	1.9409	1.9855
Knee	2.1020	2.1360	Spine	1.9317	1.9881
Side Head	2.1009	2.1430	Lung	1.9372	1.9799
X-ray Image	MEM	PSO	Ultrasonic Image	MEM	PSO
Chest	1.9136	1.9295	Baby	1.8033	1.8078
Teeth	1.9080	1.9285	Spine	1.7655	1.8336
Hand	1.8672	1.9298	Tyroid nodule	1.7814	1.8187

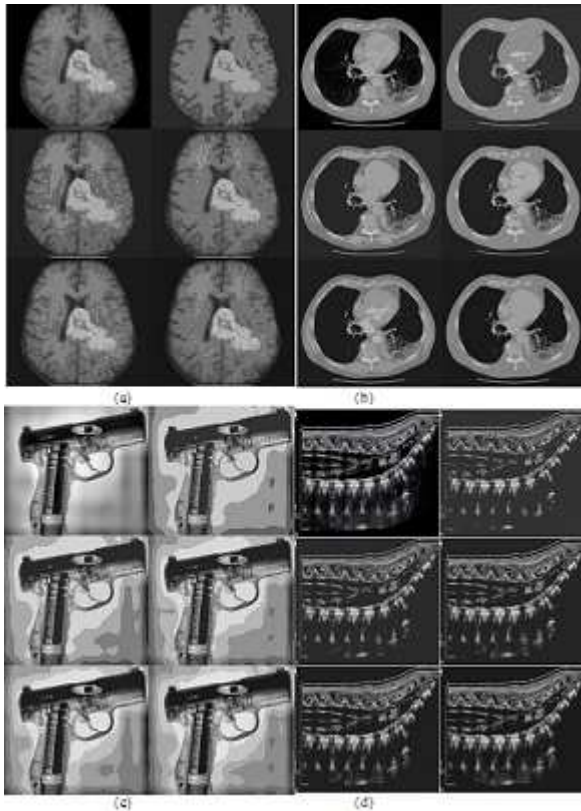


Fig. 2: Segmentation of medical images using MEM algorithm (incorporate MLE) (a) MRI Original Image(Top left), Segmented Image with cluster size $k = 4, 5, 6, 7, & 8$ are placed top right, middle left, middle right, bottom left & bottom right respectively. Likewise, (b) X-RAY Segment Image, (c) CT Segment Image & (d) Ultrasonic Segment Image.

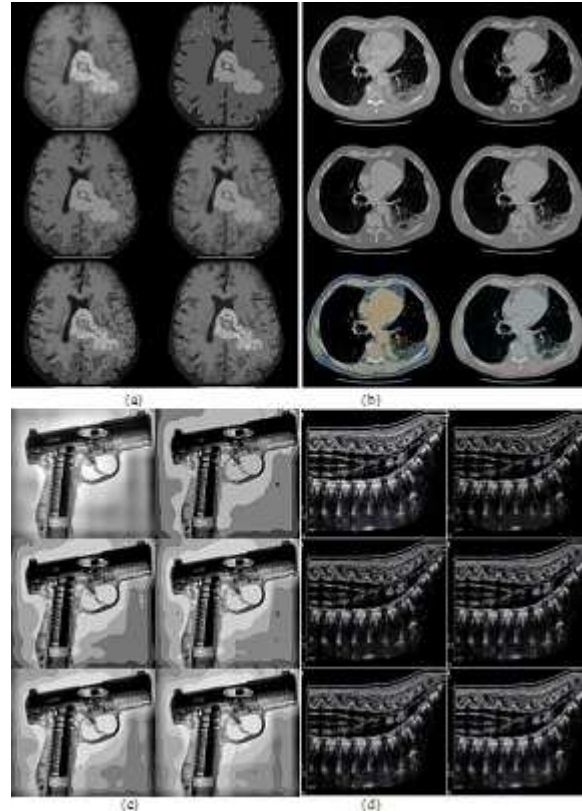


Fig. 3: Segmentation of medical images using PSO algorithm (incorporate MLE) (a) MRI Original Image(Top left), Segmented Image with cluster size $k = 4, 5, 6, 7, & 8$ are placed top right, middle left, middle right, bottom left & bottom right respectively. Likewise, (b) X-RAY Segment Image, (c) CT Segment Image & (d) Ultrasonic Segment Image.

Acknowledgement

The authors thank the Management and Principal, of Bannari Amman Institute of Technology, Sathyamangalam for providing excellent computing facilities and encouragement.

References

[1] S. Li, T. Fevens and A. Krzyzak, Automatic: clinical image segmentation using pathological modeling, PCA and SVM, Engineering Applications of Artificial Intelligence, **19**, 403-410 (2006).
 [2] A. Schwaighofer, V. Tresp, P. Mayer, A.K. Scheel and G. Muller, The RA scanner: prediction of rheumatoid joint inflammation based on laser imaging, IEEE Trans. Biomed. Imaging, **50**, 375-382 (2003).

- [3] Y. Zheng, H. Li and D. Doermann, Machine printed text and handwriting identification in noisy document images, *IEEE Transactions on Pattern Analysis Machine Intelligence*, **26**, 337-345 (2004).
- [4] W.Y. Ma and B.S. Manjunath, Edge flow: a framework for boundary detection and image segmentation, *IEEE International Conference on Computer Vision and Pattern Recognition (CVPR'97)*, San Juan, Puerto Rico, 744-749 (1997).
- [5] Chenyang Xu, L.P. Jerry, and Snakes, Shapes and gradient vector flow, *IEEE transactions on Image Processing*, **73**, 359-369 (1998).
- [6] Song Chun Zhu and Y. Alan, Region competition: Unifying snakes, region growing and Bayes/MDL for multiband image segmentation, *IEEE Transactions on Pattern Analysis Machine Intelligence*, **18**, 884-900 (1996).
- [7] D. Gatica-Perez and S. Ruiz-Correa, Extensive partition operators, gray-level connected operators, and region merging/classification segmentation algorithms, *IEEE Transactions on Image Processing*, **10**, 1332-1345 (2001).
- [8] P.K. Saha and J.K. Udupa, Optimum image thresholding via class uncertainty and region homogeneity, *IEEE Transactions on Pattern Analysis Machine Intelligence*, **27**, 689-706 (2001).
- [9] Jia-Ping Wang, Stochastic relaxation on partions with connectd components and its application to image segmentation, *IEEE Transactions on Pattern Analysis Machine Intelligence*, **20**, 619-636 (1998).
- [10] J. Xie and H.T. Tsui, Image segmentation based on maximum-likelihood estimation and optimum entropy-distribution (MLE-OED), *Pattern Recognition Letters*, **25**, 1133-1141 (2004).
- [11] G. Hamerly and C. Elkan, Alternatives to the k -means algorithm that find better clusterings, *Proceedings of 11th International Conference on Information and Knowledge Management*, 600-607 (2002).
- [12] G.H. Omran, A. Salman and A.P. Engelbrecht, Dynamic clustering using particle swarm optimization with application in image segmentation, *Pattern Analysis and Applications*, **8**, 332-344, (2006).
- [13] GuangJian Tian, Yong Xia, Yanning Zhang and Dagan Feng, Hybrid Genetic and Variational Expectation-Maximization Algorithm for Gaussian-Mixture-Model-Based Brain MR Image Segmentation, *IEEE transactions on information technology in biomedicine*, **15**, 373-380, (2011).
- [14] Yifeng Zhou and Jim P.Y. Lee, A Modified Expectation Maximization Algorithm for Maximum Likelihood, *IEEE Conference on Signals, Systems and Computers*, 613-617 (2000).
- [15] Xian Jinlong, Li Jianwu and Yang Yang, A New EM Acceleration Algorithm for Multi-user Detection, *IEEE International Conference on Measuring Technology and Mechatronics Automation*, **1**, 150-153 (2011).
- [16] J. Kennedy and R. Eberhart, Particle swarm optimization, *Proceedings of the IEEE International Conference on Neural Networks*, Perth, Piscataway, NJ, 1942-1948 (1995).
- [17] John Canny, A Computational Approach to Edge Detection, *IEEE Transactions on Pattern Analysis and Machine Intelligence*, **8**, 679-698 (1986).
- [18] Ahmet M. Eskicioglu and Paul S. Fisher, Image Quality Measures and their performance, *IEEE Transactions on Communications*, **43**, 2959-2965 (1995).
- [19] Marta Mrak, Sonja Grgic and Mislav Grgic, Picture Quality Measures in Image Compression Systems, *EUROCON 2003*, Ljuijana, Slovenia.
- [20] Ismail Avicibas, Bulent Sankur and Khalid Sayood, Statistical Evaluation of Image Quality Measures, *Journal of Electronic Imaging*, **11**, 206-223 (2002).
- [21] Zhou Wang, Alan Conrad Bovik., et.al., Image Quality Assessment: From Error Visibility to Structural Similarity, *IEEE Transactions on Image processing*, **13**, 600-612 (2004).
- [22] Gleb Beliakov and Jim Warren, Appropriate choice of aggregation operators in Fuzzy decision systems, *IEEE Transactions on Fuzzy Systems*, **9**, 773-784 (2001).
- [23] Ronald R. Yager, Including importance in OWA Aggregations using Fuzzy systems modeling, *IEEE Transactions on Fuzzy Systems*, **6**, 286-294 (1998).



R. Harikumar received his B.E (ECE) Degree from REC (NIT) Trichy 1988. He obtained his M.E (Applied Electronics) degree from College of Engineering, Guindy, Anna University Chennai in 1990. He was awarded Ph.D. in I & C Engg from Anna university Chennai in 2009. He has 24 years of teaching experience at college level. He worked as faculty at Department of ECE, PSNA College of Engineering & Technology, Dindigul. He was Assistant Professor in IT at PSG College of Technology, Coimbatore. He also worked as Assistant Professor in ECE at Amrita Institute of Technology, Coimbatore. Currently he is working as Professor ECE at Bannari Amman Institute of Technology, Sathyamangalam. He has published eighty one papers in International and National Journals and also published around more than hundred papers in International and National Conferences conducted both in India and abroad. His area of interest is Bio signal Processing, Soft computing, VLSI Design and Communication Engineering. He is guiding nine PhD theses in these areas. He is life member of IETE, ISTE, and member IEEE.



B. Vinoth Kumar received his B.E (EEE) degree from Bannari Amman Institute of Technology, Sathyamangalam, Bharathiar Uuniversity, Coimbatore in 2002. He obtained his M.E (Applied Electronics) degree from Government College of Technology, Coimbatore in

2005. He has nine years of teaching experience at college level. Currently he is working as Assistant Professor (Senior Grade) in Department of EEE at Bannari Amman Institute of Technology, Sathyamangalam. His area of interest is Medical Image Processing, Soft computing, and Pattern recognition.